Effects of climate change on the intensity and frequency of heavy snowfall events in the Pyrenees

López-Moreno, Juan Ignacio; Goyette, Stéphane; Vicente-Serrano, S. M.; Beniston, Martin

Climatic Change (2011) 105:489–508
DOI 10.1007/s10584-010-9889-3

Effects of climate change on the intensity and frequency of heavy snowfall events in the Pyrenees

Juan Ignacio López-Moreno · S. Goyette · S. M. Vicente-Serrano · M. Beniston

Received: 16 January 2009 / Accepted: 2 June 2010 / Published online: 17 August 2010

Abstract The intensity and frequency of heavy snowfall events in the Pyrenees were simulated using data from the HIRHAM regional climate model for a control period (1960–1990) and two greenhouse emission scenarios (SRES B2 and A2) for the end of the twenty-first century (2070–2100). Comparisons between future and control simulations enabled a quantification of the expected change in the intensity and frequency of these events at elevations of 1,000, 1,500, 2,000 and 2,500 m a.s.l. The projected changes in heavy snowfall depended largely on the elevation and the greenhouse gas emission scenario considered. At 1,000 m a.s.l., a marked decrease in the frequency and intensity of heavy snowfall events was projected with the B2 and A2 scenarios. At 1,500 m a.s.l., a decrease in the frequency and intensity is only expected under the higher greenhouse gas emission scenario (A2). Above 2,000 m a.s.l., no change or heavier snowfalls are expected under both emission scenarios. Large spatial variability in the impacts of climate change on heavy snowfall events was found across the study area.

1 Introduction

It is widely recognized that, amongst the components of the earth system, snow and ice are likely to be the most sensitive to climate variability and change (Wash 1995; Nesje and Dahl 2000; Carrivick and Brewer 2004). In recent years there has been marked scientific interest in assessing how the shifts in climate expected in coming decades will impact on snowpack. Most previous studies have focused on potential

J. I. López-Moreno (✉) · S. M. Vicente-Serrano
Instituto Pirenaico de Ecología, CSIC, Campus de Aula Dei, P.O. Box 202, Zaragoza, 50080, Spain
e-mail: nlopez@ipe.csic.es

S. Goyette · M. Beniston
C3i, Climatic Change and Climate Impacts Group, University of Geneva, Batelle/D, 7 Chemin de Drize, 1227 Carouge (Geneva), Switzerland

changes in the accumulated snowpack in cold and mountain regions. This is of interest because snow controls numerous environmental and ecological processes (Mellander et al. 2007; Jonas et al. 2008a, b), determines the amount of water available for urban and agricultural water supply and hydropower production, and affects the potential development of economic activities such as those related to winter tourism (Beniston 2003; Barnett et al. 2005; Lasanta et al. 2007; Uhlmann et al. 2009). However, much less attention has been paid to potential changes in extreme snowfall events. These can disrupt traffic (Datla and Sharma 2008), cause large economic (e.g. collapse of infrastructure) and environmental damage as consequence of the heavy loads of accumulated snow (Strasser 2008), result in injuries and fatalities related to traffic accidents, and increase the frequency of avalanches (Spreitzhofer 2000; Changnon and Changnon 2006; Germain et al. 2009; Beniston et al. 2003; Höller 2009). Moreover, heavy snowfall followed by melting can trigger large floods that constitute an additional major natural hazard (Changnon and Changnon 2006).

The Pyrenees region is subject to heavy snowfall events that affect villages, disrupt transportation, and trigger snow avalanches that damage villages, infrastructure, ski resorts and forests; there is an upward trend in the number of injuries and fatalities that occur each year, as a consequence of an increase in the popularity of outdoor winter activities (Julian-Andrés et al. 2000; Esteban et al. 2005). Heavy snowfall at 1,000–1,500 m a.s.l. in the Pyrenees region has major implications for traffic planning, affects the inhabitants of high-elevation villages, causes economic losses through damage to infrastructure, and can limit access to ski resorts and their operation. Heavy snowfall at higher elevations (2,000–2,500 m a.s.l.) causes damage to vegetation and fauna, and can trigger large avalanches reaching inhabited settlements and areas where infrastructure is located, significantly amplifying their consequences.

Previous studies have predicted an increase in temperature for the region (López-Moreno et al. 2008a), leading to a decrease in snowpack accumulation and duration that will be particularly marked at lower elevations (López-Moreno et al. 2009). Projections also suggest that the region will be subject to an intensification of precipitation extremes, with a generalized trend of increase in daily intensity, and an increasing contribution of intense events to total precipitation (López-Moreno and Beniston 2009). In this context the evolution of snow-related extreme events is highly uncertain, and is of outstanding scientific and applied interest.

As global temperature is expected to increase in coming decades, most previous regional studies have highlighted the likelihood of a sharp decrease in accumulated snowpack, a shortening of the snow-cover season, and a decreased and earlier spring freshet (Rasmus et al. 2004; Dankers and Christensen 2005; Keller et al. 2005; Merritt et al. 2006; Hantel and Hirtl-Wielke 2007; Mellander et al. 2007). However, there are few estimates of the potential changes in heavy snowfall events (HSEs) as a consequence of projected climate change. The temporal evolution of damaging snow storms shows that warmer average temperatures do not necessarily reduce heavy snowfall. Thus, Changnon (2007) reported a lower frequency but higher intensity of winter storms in the USA during the twentieth century. For the Swiss Alps, the frequency of HSEs was constant or increased slightly for the period 1933–1999, despite a marked decrease in snow depth and duration at mid-to-low elevations, as a consequence of warmer temperatures (Laternser and Scheebeli 2003). In this context it is not clear what impact a changing climate will have on heavy snowfall, particularly when precipitation extremes are expected to increase with increasing concentrations of greenhouse gases in the atmosphere (Kim 2005; Frei et al. 2006; Gao et al. 2006). In the present study, we analyze the expected changes in HSEs projected by using the HIRHAM model for the Pyrenees in the twenty-first century. Snow-depth evolution was simulated using a Surface Energy Balance Model (GRENBLS) including and explicit snow module for a control period (1960–1990) and a future (2070–2100) period under two greenhouse gas emission scenarios (the IPCC SRES B2 and A2 scenarios; Nakicenovic et al. 1998). Simulations were conducted for 20 individual grid points throughout the Pyrenees at four elevations (1,000, 1,500, 2,000 and 2,500 m a.s.l.), enabling an assessment of the expected changes including horizontal spatial variability and altitudinal gradients. Snowfall on individual days, the total snow accumulated during a multi-day snowfall period, and the number of days and multi-day snowfall events over 30 and 60 cm, respectively, were considered in the analysis of changes in HSEs.

2 Study area

The study area is the Pyrenean mountain range, bounded by the Mediterranean Sea to the east and the Atlantic Ocean to the west (Fig. 1). Large areas lie above 1,000 m a.s.l. and summits may exceed 3,000 m a.s.l.

The Pyrenees are subject to an eastward transition in climate from Atlantic to Mediterranean conditions. Moreover, the relief causes marked variability in precipitation and temperature distributions. In the Central Ebro Depression the average annual precipitation is approximately 300 mm and the average annual temperature is 13–15°C. In the mountains, annual precipitation exceeds 600 mm, reaching 2,000 mm

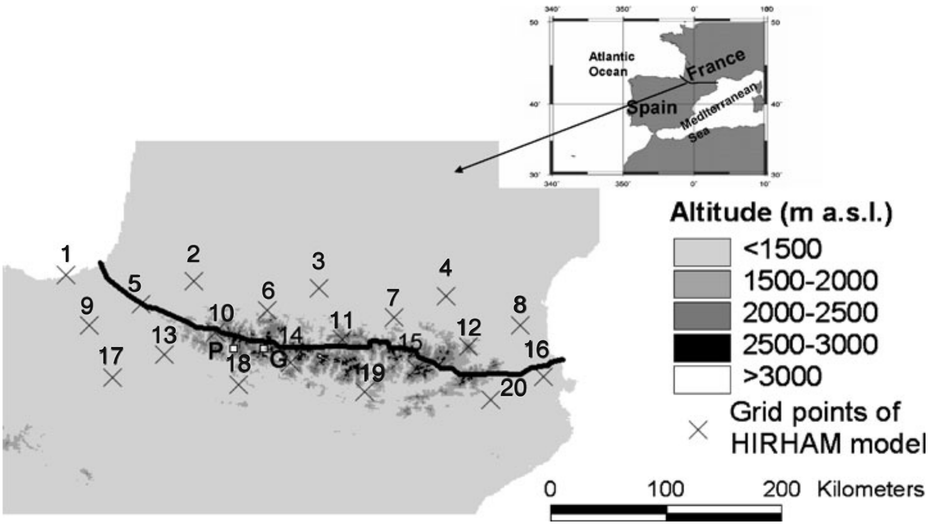

Fig. 1 Map of the study area. *Circles* indicate the grid points from the HIRHAM model used for simulating snowpack evolution. The *squares* indicate the location of the stations used for validation; *P* Panticosa station; *G* Góriz station

at the highest elevations (Cuadrat et al. 2007). Most precipitation falls as snow during winter in the Atlantic areas, and during spring and autumn in the Mediterranean regions. Summers are generally relatively dry in the Pyrenees, and very dry in the Ebro Depression. Extreme precipitation events in the Pyrenees can occur at any time, but they tend to occur most frequently during winter and spring in Atlantic areas, and during autumn in Mediterranean areas (Beguería et al. 2009).

Temperature is strongly controlled by altitudinal gradients, and is estimated to vary by 0.63°C per 100 m elevation change (López-Moreno 2006). Between November and April the 0°C isotherm is approximately 1,600 m a.s.l. (García-Ruiz et al. 1986), representing the level above which snow accumulates over a long period. Below, a thin snowpack generally only appears during the coldest winter months (December to February); at 1,000 m a.s.l. there is no permanent snowpack but frequent snowfalls may occur. A snowpack of 2–4 m in depth develops above 2,000 m a.s.l. and lasts until the end of May, or June on upper and shaded slopes (López-Moreno 2005; López-Moreno et al. 2007).

3 Data and methods

The time evolution of a snow cover is well described with land-atmosphere water and energy exchanges. Such processes, expressed in terms of water and energy budgets, are computed in a surface energy balance model (SEBM) termed GRENBLS (details found in Keller et al. 2005; Keller and Goyette 2005; López-Moreno et al. 2008b). This model is similar to a land surface model formulation of intermediate complexity such as those in Global and Regional Circulation Models (GCMs and RCMs), but it differs in the details. Such simple models have shown genuine skill in reproducing the time duration and depth of a number of seasonal snowpack and compare generally well with more complex snow schemes, without bearing their computational load (i.e., Boone and Etchevers 2001; Etchevers et al. 2003). Complex snow model are mainly used to study the physical properties of snow, to predict avalanches (Brun et al. 1992) or for hydrological forecasting (Brun et al. 1997). In the present context, a single-layer snow module included in a SEBM is therefore preferred. GRENBLS has a tiled surface structure including a distinct snow layer. The model is a physically-based semi-prognostic model driven by hourly input data of air temperature, T_a (K), dew point temperature, T_d (K), anemometer-level wind magnitude, W_s (m s^{-1}), precipitation, P (mm s^{-1}), and surface pressure, p_{sfc} (h Pa). The model computes the radiative fluxes (although incoming solar radiation, $K\downarrow$ (W m^{-2}), is prescribed in this study), the surface turbulent sensible and latent fluxes, as well as the heat flux in the ground and in the snowpack. Ground and snow temperatures, soil wetness and snow mass are prognostic variables. Snow is modelled as an evolving one-layer pack characterised by a temperature, a mass in terms of the snow water equivalent, SWE (kg m^{-2}), and a density. The energy change associated with the melting of frozen soil moisture and snow is taken into account. The water budget at the surface is also calculated using separately the liquid and solid phases of water. Precipitation is considered as solid if T_a is lesser than that of the triple point of water. Liquid precipitation on a snowpack induces snowmelt. Melted water goes directly into the soil as liquid moisture. The surface energy budget is computed at each model time step over snow cover. If the heat storage is positive and the snow temperature below the melting point, the excess energy is first used to raise the temperature of the pack. Once its temperature reaches the melting point, any additional excess energy is the used to melt the snow. The temperature of the snow is held below the melting point until the snow has melted. The melted snow goes directly into the ground as liquid moisture.

Snow water equivalent and snow depth evolution were simulated for 20 individual points throughout the Pyrenees (Fig. 1) with climate inputs provided by the HIRHAM regional climate model (RCM) on a daily basis and at a spatial resolution of 0.5° (Christensen et al. 1998) for the control and late twenty-first century periods under the A2 and B2 scenarios. The RCM outputs are made available daily from the EU-PRUDENCE project (http://prudence.dmi.dk). The scenarios for 2070–2100 reflect two contrasting hypotheses of the evolution of greenhouse gas emissions (SRES A2 and B2) related to economic and demographic behavior by 2100. A2 is characterized by higher emissions than B2 (IPCC 2007; Nakicenovic et al. 1998).

López-Moreno et al. (2008b) demonstrated that simulated change in snow accumulation and melting in a location of the Pyrenees were consistent among nine different RCMs from the PRUDENCE dataset. For this reason, it was preferred to present analyses based on a single RCM simulation (HIRHAM model) instead of a RCMs-ensemble, since this would undoubtedly lead to larger uncertainties (and/or dispersion) in the pooled results.

Prior to snowpack simulations the climatic series had to be disaggregated from daily to hourly data, and scaled to the four elevation levels (1,000, 1,500, 2,000 and 2,500 m a.s.l.). Temperature, precipitation, and dew point temperature were scaled by means of the application of daily elevation adjustment rates. Atmospheric pressure is adjusted to different altitudinal planes by applying the following barometric correction (Berberan-Santos et al. 1997):

$$p_{sfc} = \mathrm{p_{obs}}\left(\frac{T_{air}}{T_{air} + \gamma\ \Delta z}\right)^{\frac{g}{R_d \gamma}} \tag{1}$$

where T_{air} is the observed temperature (K), $\mathrm{p_{obs}}$ is the atmospheric pressure ($\mathrm{p_{sfc}}$) at the grid point altitude, Δz is the altitude difference, γ is a mean vertical lapse rate defined as −6.5 K/km, g is gravitational acceleration (9.81 m $\mathrm{s^{-1}}$), and $\mathrm{R_d}$ is the specific gas constant for dry air (287.04 J $\mathrm{kg^{-1}}$ $\mathrm{K^{-1}}$). Given a lack of appropriate data and absence of clear altitudinal trends in simulated wind speed, we consider it invariant with altitude. Daily HIRHAM climatic data were disaggregated into hourly series following different procedures and assumptions. For temperature data, a cosine function was adjusted to daily maximum and minimum temperature via the following analytical equation (see Jansson and Karlberg 2001):

$$\mathrm{T_a(t)} = \mathrm{T_{mean}} - \mathrm{T_{amp}}\cos\left(\frac{\mathrm{t} - \mathrm{t_{ph}}}{\mathrm{y_{cycle}}}2\pi\right) \tag{2}$$

where t represents the time in hour, $T_a(t)$ is air temperature, T_{mean} is the mean daily temperature, T_{amp} is the daily amplitude in temperature ($T_{max} - T_{min}$), t_{ph} is the phase shift in air temperature (2,400 when a diurnal cycle is assumed), and y_{cycle} is the air temperature cycle (24 h). At each grid point, cloudiness (C), wind speed (W_s), and surface pressure (p_{sfc}) were assumed to change linearly from one day to the next, in an hourly fashion. Surface pressure (p_{sfc}) is then estimated for different iso-altitude planes via barometric correction (Eq. 2), using temperature data disaggregated in hourly series with Eq. 3. Total daily precipitation was divided by 24 and shared equally throughout the day. Dew point temperature was dissagregated using hourly temperature obtained from the cosine function (Eq. 2) and psychometric equations (Perry and Green 1997; Hallcross 1997) that relate temperature with vapor pressure changes. A full description of the methods, the transformation of the original climate series, and their further validation can be found in López-Moreno et al. (2009).

The GRENBLS outputs considered in this study were snow depth series at hourly intervals for the 20 points and the four elevation levels. The snow depth series were simplified into daily series based on the snow depth valid at noon and, by means of the daily difference, were converted into daily accumulation or ablation series. From these series snowfall events were identified as those periods when snow depth increased at least 5 cm per day. A day without snowfall (or <5 cm) was used to distinguish snowfall events. Data were extracted on the maximum amount of snowfall during a single day (maximum snowfall) per snowfall event, and the fresh snow accumulation during multi-day snowfall events. In addition, we followed an approach based on partial duration (PD) series, which is commonly used in statistics for extreme values (Hershfield 1973). Based on a given threshold (x_0), the number days with snowfall exceeding 30 cm (HSE), and multi-day snowfall accumulations over 60 cm (heavy accumulation events; HAE) were considered. A threshold of 30 cm in 24 h is considered sufficient to trigger avalanches in the Pyrenees (Esteban et al. 2005) and to severely disrupt traffic, whereas an accumulation of 60 cm of fresh snow leads to a generalized risk of avalanche, and indicates a snow load with the potential for damaging infrastructure and vegetation (McClung and Schaerer 1993).

As demonstrated by Beguería (2005), the series generated by exceedances over a threshold (PD series) tend to converge to a generalized Pareto (GP) distribution. In the form commonly applied to PD series, the GP distribution is described by a shape parameter κ and a scale parameter α, and has the following cumulative distribution function:

$$f(x) = \frac{1}{\alpha}\left[1 - \frac{k}{\alpha}(x - \varepsilon)\right]^{1/k-1}, \tag{3}$$

where x is the maximum daily snowfall exceeding 30 cm or multi-day snowfall accumulation over 60 cm, and ε is a location parameter or distribution origin that corresponds to the lowest value of the series of x. The parameters of the distribution are readily estimated from the L-moments of the data series (Hosking 1990):

$$\alpha = \lambda_1\left(\frac{1}{\tau} - 1\right), \tag{4}$$

$$\kappa = \frac{1}{\tau} - 2, \tag{5}$$

where λ_1, λ_2 are the first two probability-weighted moments and $\tau = \lambda_2/\lambda_1$. Rao and Hamed (2000) provides further details on the calculation of L-moments.

The L-moment ratio diagrams (see Hosking 1990) confirmed that the series of snowfall events at the various elevations for the control and future scenarios closely matched the GP distribution (Fig. 2), as has been widely observed for most

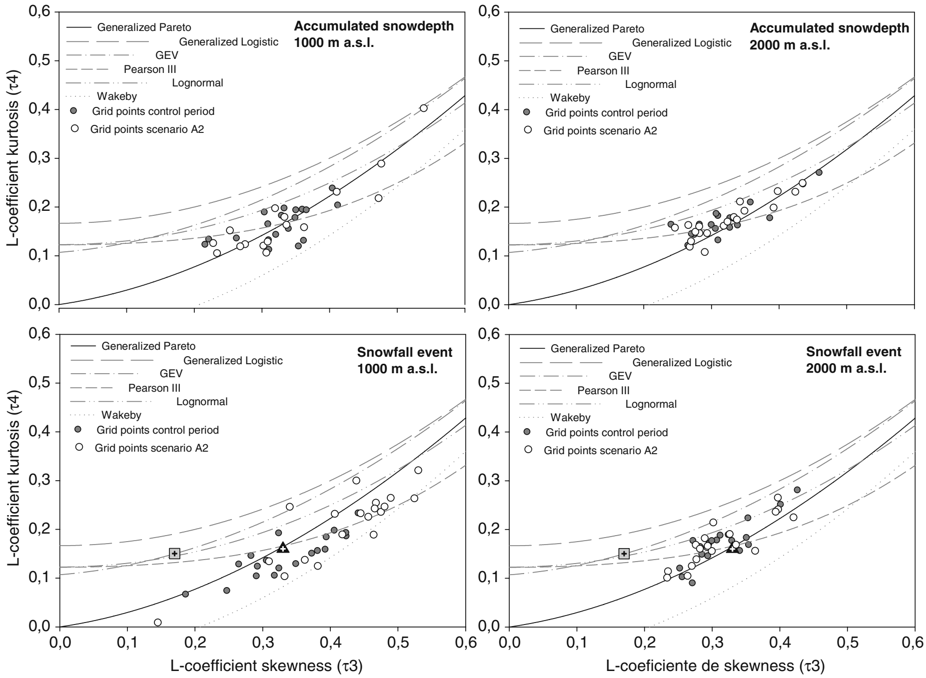

Fig. 2 L-moments diagram for the series of maximum intensity in a single day snowfall event above 30 cm, and total snow accumulated above 60 cm during a multi-day snowfall event at 1,000 and 2,000 m a.s.l. for the control period and the A2 emission scenario

extreme hydrological variables (Hosking and Wallis 1987; Madsen and Rosbjerg 1997; Beguería 2005).

According to the GP distribution, the maximum expected (or quantile) snowfall or snowfall accumulation X_T over a period of T years is derived as follows:

$$X_T = \varepsilon + \frac{\alpha}{\kappa}\left[1 - \left(\frac{1}{\lambda T}\right)^{\kappa}\right],$$

where λ (as distinct from the probability weighted moments, λ_1 and λ_2) is the average annual number of events above the threshold (x_0). Quantiles for a recurrence of 2-year and 25-year return periods were calculated from the maximum snowfall and snow accumulated in multi-day snowfall events for each grid point at the various iso-elevation planes for SRES B2 and A2, and compared to those obtained for control runs. This procedure enabled quantification of the expected change in HSEs across the Pyrenees by the end of the twenty-first century.

Assessment of the reliability of indicators related to HSEs from RCM outputs is difficult. The main difficulties in validation are: (1) the different spatial scales of the RCM gridded data (at a resolution of 0.5° ≈ 50 km at 42°N) and the information from local meteorological stations, (2) the mismatch between the center of the RCM and the location of the stations, (4) the marked spatial variability of snowpack over short distances as a consequence of topography and wind redistribution, and (4) the

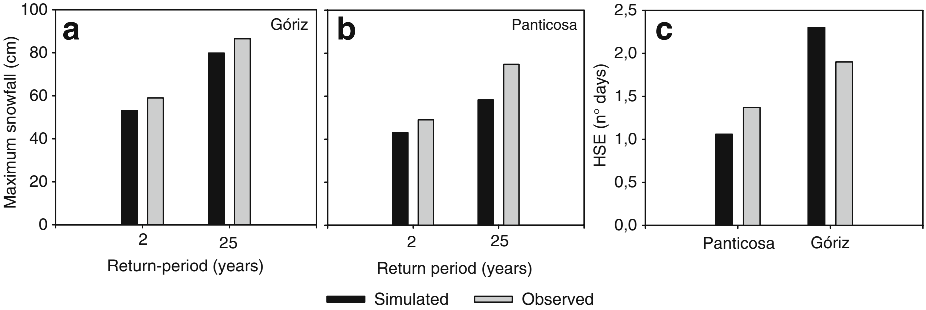

Fig. 3 2-year and 25-year quantiles for the intensity of snowfall events (in a single day) for the control period (average of grid points 6, 10, 14 and 18) and for the stations at Panticosa (**a**) and Góriz (**b**), and the number of simulated and observed HSEs exceeding 30 cm (**c**)

paucity of long-term records of snowpack in the study area. With respect to the latter, none cover the full control period as most of the stations were installed during the last decade. Within the context of these limitations, Fig. 3 compares the 2-year and 25-years quantiles corresponding to snowfall in a single day (Fig. 3a, b, respectively) and the number of events per year exceeding 30 cm of snow depth (Fig. 3c), obtained from snowpack data between 1982 and 2000 for two instrumented stations located at 1,630 and 2,200 m a.s.l., and data simulations for the control period obtained from the HIRHAM model for the same elevations. The simulated data were derived by averaging the four grid points that bound the stations (grid points 6, 10, 14 and 18 in Fig. 1). Despite some discrepancies between the predicted and observed data that are always to be expected, the RCMs effectively simulated intense snowfall events. In general a slight underestimation was observed in the simulated values, except for HSEs in Góriz, where some overestimation occurred. These results are consistent with previous findings of the capacity of RCMs to simulate seasonal precipitation and temperature over the Pyrenees (López-Moreno et al. 2008a), magnitude heavy precipitation events and their contribution to total precipitation (López-Moreno and Beniston 2009) and snowpack evolution (López-Moreno et al. 2008b, 2009). The HIRHAM RCM applied to this study has in the past shown genuine skill in reproducing extreme events, in particular anomalously warm winter periods in the Alps (Beniston 2005) and catastrophic rainfall events (Beniston 2006), thereby providing some measure of confidence in its capacity for simulating changes in means and extremes in a scenario climate. However, there were some limitations in the data used, indicating the need for caution in interpretation of the results.

4 Results

Figure 4 shows two box plots for the 2-year and 25-year quantiles of the maximum snowfall per event, corresponding to the 20 analyzed grid points under the control and future scenarios at the four elevation levels. Table 1 shows the simulated percent change under the B2 and A2 scenarios relative to the control period. At 1,000 m a.s.l., the intensity of HSEs is expected to decrease markedly under the A2 scenario, with a mean reduction of 51% and 32% for events corresponding to the 2-year and

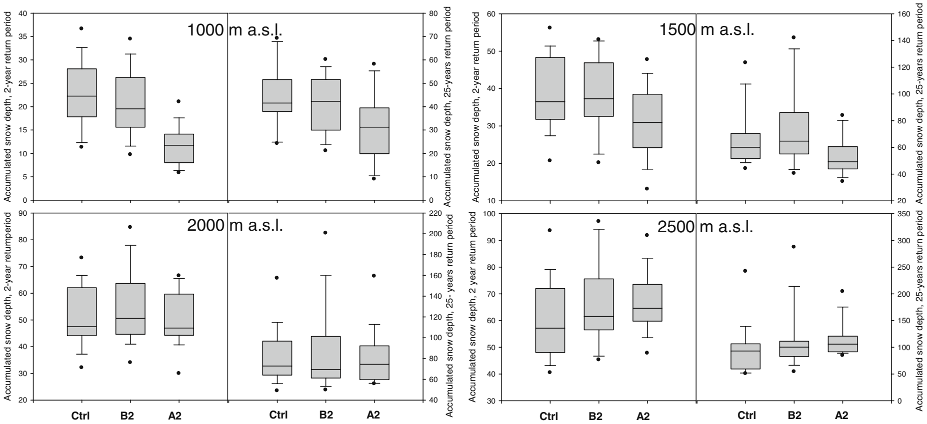

Fig. 4 Box plots for the 2-year and 25-year quantiles of the maximum snowfall in a single day for a return period of 1 and 25 years at various elevations for the control period and for the B2 and A2 emission scenarios. The *central line* indicates the average of the 20 analyzed grid points. *Boxes* indicate the 25 and 75 percentiles, *whiskers* indicate the 10 and 90 percentiles, and *dots* indicate the 5 and 95 percentiles

25-year quantiles, respectively. Under the B2 scenario, the decrease is 10% and 5%, respectively. At 1,500 m a.s.l., HSEs corresponding to the 2-year and 25-year quantiles are expected to decrease under scenario A2, with a mean reduction of 22% and 16%, respectively, and to remain stationary under the B2 emission scenario. Little change is expected at 2,000 m a.s.l., and the most intense snowfall events at this elevation are likely to increase markedly in the higher areas (22% and 32% under A2 scenario conditions for the most extreme 25-year quantile events).

The results reflect the mean changes simulated for the entire area, but the spatial differences across the study area are noteworthy. Figure 5 shows the spatial distribution of the 25-year quantile for the maximum intensity of snowfall for the control period and the A2 scenario at 1,000 and 2,000 m a.s.l. During the control period at 1,000 m a.s.l., at least one event is expected with snowfall greater than 40 cm in 25 years in the northern sector of the range, and even more such events are expected in areas close to the Atlantic Ocean and Mediterranean Sea. In the southern sector of the range, these events generally range from 20 to 40 cm. Under the A2 scenario, the maximum 25-year snowfall intensity generally ranges from 20 to 40 cm in northern parts, whereas in the south it ranges from 10 to 30 cm. Comparison of the control and A2 scenarios reveals that greater decreases in snowfall intensity are expected in the most southern sectors of the study area, where snowfall intensity may decline 50% or more. The expected decrease is less marked in the north, ranging from −5% to −15%. The projected changes for 2,000 m a.s.l. are quite different, with the maximum 25-year quantile snowfall intensities generally ranging from 50 to 100 cm in a single day for both the control and the A2 scenario, with a moderate increase in the values in central areas of the range. A decrease in the maximum 25-year quantile snowfall, generally not more than −20%, is expected in various sectors, and a near stationary evolution is also expected for large areas.

Very similar results were obtained for total snow accumulated during multi-day events. Figure 6 shows that a significant decrease in the maximum expected

Table 1 Simulated change (in percentage) of intensity of maximum snowfall event (single day) and maximum snow accumulation during a multi-day snowfall event for a recurrence of 2 and 25 years under B2 and A2 scenarios with respect control period

Grid point	Maximum snowfall event															
	1,000 m a.s.l.				1,500 m a.s.l.				2,000 m a.s.l.				2,500 m a.s.l.			
	B2		A2		B2		A2		B2		A2		B2		A2	
	1.0	25.0	1.0	25.0	1.0	25.0	1.0	25.0	1.0	25.0	1.0	25.0	1.0	25.0	1.0	25.0
1	−2.2	−23	−48.8	−15.8	−6.1	−29	−13.8	−50.6	6.1	3.1	−1.5	−2.1	3.3	2.7	0.0	6.2
2	−9.7	−8.5	−54.8	−32	−7.6	−1.5	−22.8	−23.8	0.9	7.7	−6.0	−11	8.6	9.5	3.1	−2.2
3	1.9	−17.6	−35.8	−19.9	3.8	−10.9	−24.5	−11.8	4.2	8.4	0.6	2	2.8	10.8	8.8	21.5
4	−14.7	−4.4	−65.6	−69	−9.5	15.2	−27.9	−30	−0.6	−17.4	−8.0	−10.3	−1.7	−8	7.4	59.8
5	−12.6	13.4	−56.4	−26.2	−3.5	−1.9	−18.8	−21.3	0.2	−4.7	−5.0	−11	5.6	−3.3	1.3	−6.9
6	−13.5	−15	−39.7	−29.8	3.3	10	−13.3	6.1	3.2	−7.2	1.9	−9.3	11.7	57.2	12.0	62.8
7	−6.8	13.4	−44.3	−57	−6.3	2.3	−33.7	−33	8.0	−26	5.9	−0.6	8.2	−11.4	14.5	66.0
8	−18.4	−34.8	−38.2	−25.1	−46.4	−44.5	−27.4	−18.8	3.4	6.0	−7.5	28.5	8.9	23.4	10.8	41.5
9	−5.4	−5.6	−51.2	−20.5	−0.1	46.8	−7.5	11.4	5.0	−10.7	−0.3	−10.0	5.1	−20	4.5	−13
10	−15.7	38.0	−50.8	−15.4	−10.7	11.1	−24.3	−23	−0.8	−28.3	−5.7	−32.8	−25.2	−9.9	6.2	13.7
11	−0.6	0.1	−47.8	−56	−5.2	43.6	−24.2	−6.1	9.9	0.3	−1.3	−16	10.9	54.5	19.7	85.5
12	−20.4	−15	−53.8	−63.8	−5.	2	−35.9	−21.8	4.7	6.7	−10.4	0.1	12.7	5.5	12.7	31.4
13	−17.9	−6.7	−56.8	−36.9	7.8	9.4	−26.5	−24.3	0.0	−15.8	−0.5	0.3	16.6	60.1	11.1	63.5
14	5.3	−10.6	−35.9	−23.7	4.5	7.0	−24.9	−11.3	18.5	19.5	8.3	13.6	20.7	82.3	12.7	80.6
15	−2.6	8.4	−53.6	−27.6	−6.8	43.3	−25.0	5.8	7.4	20.2	7.3	−24.1	9.2	6.6	12.0	13.3
16	−29.7	−17.7	−76.8	−57	−9.8	2.3	−37.2	−32	0.2	7.3	−12.7	5.0	0.9	−8.5	1.4	11.1
17	−14.6	12.1	−53.0	−4	9.1	31.0	−13.2	−7	−0.8	26.3	2.2	0.4	14.4	10.4	6.6	−4.0
18	3.5	0.0	−34.6	−23.8	19.1	−1.2	−7.2	5.3	22.0	−5.2	10.9	22.0	25.1	103	19.0	98.0
19	−12.0	−18.7	−58.5	−22.8	−3.6	27.4	−19.7	−22.9	19.5	42.9	−0.5	41.0	15.2	59.3	10.4	46.7
20	−16.7	−12.9	−54.3	−15.9	−9.2	49.9	−21.4	−13.8	11.7	28.9	−7.7	−27	−1.8	17.6	−7.9	−27.4
Average	−10	−5	−51	−32	−4	11	−22	−16	6	3	−1	−2	8	22	8	32

Table 1 (continued)

Grid point	Accumulated depth in a multiple-day snowfall															
	1,000 m a.s.l.				1,500 m a.s.l.				2,000 m a.s.l.				2,500 m a.s.l.			
	B2		A2		B2		A2		B2		A2		B2		A2	
	1	25	1	25	1	25	1	25	1	25	1	25	1	25	1	25
1	−6.8	−5.8	−17.2	−49	2.2	5.3	−12.3	−19	7.4	−3.5	0.78	1.27	−9.6	−0.1	−5.1	−6.4
2	1.2	−8.2	−43.7	−53	−24.4	1.9	−2.5	−24.0	7.0	−2.8	−2	8.46	13.5	7.31	22.7	−15
3	8.3	0	−33.3	−56	−25.0	8.0	9.6	−23.1	−6.0	−0.4	−3.6	7.25	2.17	9.54	8.88	36.7
4	−7.8	−6	−64.0	−74	−27.7	0	3.0	−28.3	−0.5	−8.7	7.09	5.32	8.58	11.4	30.8	46.6
5	6.9	−3.7	−39.9	−52	−5.7	5.6	19.7	−21	21.2	−1.3	14.7	10.5	17	11.4	47.6	30.8
6	16.7	7.3	−5.7	−64	4.0	6.3	24.2	−8.6	13.7	8.62	3.48	11.8	21.4	19.4	27.2	10.7
7	−15.5	−2.3	−51.7	−60	−26.7	5.8	−6.1	−32	−19.9	7.29	−1	13.5	13.7	21.1	10.7	−22
8	−29.4	−47.4	−16.6	−48	−39.6	0.1	−46.6	−25	−3.4	−12	0.71	4.89	32.6	7.45	46.6	18.7
9	−4.0	3.2	−44.1	−47	15.7	6.0	2.9	−12.0	10.1	−3.9	0.22	6.85	15.3	1.12	−4.5	36.5
10	48.7	−2	−3.7	−53	−6.2	−2.7	22.5	−26	−4.5	−7.8	−9.8	−21	−1	5.64	4.55	17.3
11	−9.5	−4.0	−39.3	−56	−35.5	13.1	6.1	−24	16.3	−3.2	2.33	8.35	20.9	16.4	36.5	0.34
12	−28.6	−7.9	−61.2	−55	−15.3	6.4	−4.9	−34.3	1.8	−7.9	13.6	17	2	16.7	36.7	27.2
13	−22.7	3.3	−31.0	−59	−27.0	1.0	−3.7	−24	23.5	−2.9	20.5	9.61	22.4	9.83	28.5	32.2
14	−32.8	9.4	−34.0	−38	−31.0	14.8	1.6	−19.0	16.4	2.41	18.5	17.9	36.1	8.57	17.3	−5.1
15	−9.0	−12.0	−40.2	−60	−30.7	4.5	10.7	−32	19.4	−2.1	5.56	7.62	14.5	7.54	18.7	−4.5
16	−19.0	−13.4	−55.3	−87	−35.1	0.3	3.7	−41.1	−7.0	−16	−19	5.26	4.25	−0.9	−6.4	47.6
17	0.3	9.3	−6.5	−55	−5.1	−6.1	27.5	−18	13.9	0.97	11.3	15.8	19.7	14.7	32.2	22.7
18	−13.5	17.4	−36.2	−37	−26.6	19.0	−8.0	−11.4	6.9	5.53	15	16.4	23.7	10.6	0.34	8.88
19	−3.1	−8.8	−12.5	−67	−25.4	11.4	11.1	−28.8	14.6	−7	−31	11.3	16.8	2.95	−22	4.55
20	−12.6	−8.9	−25.4	−64	−32.5	6.1	26.1	−28.8	16.9	−16	−32	3.1	24	−12	−15	28.5
Average	−7	−4	−33	−57	−20	5	4	−24	7	−3	1	8	15	8	16	16

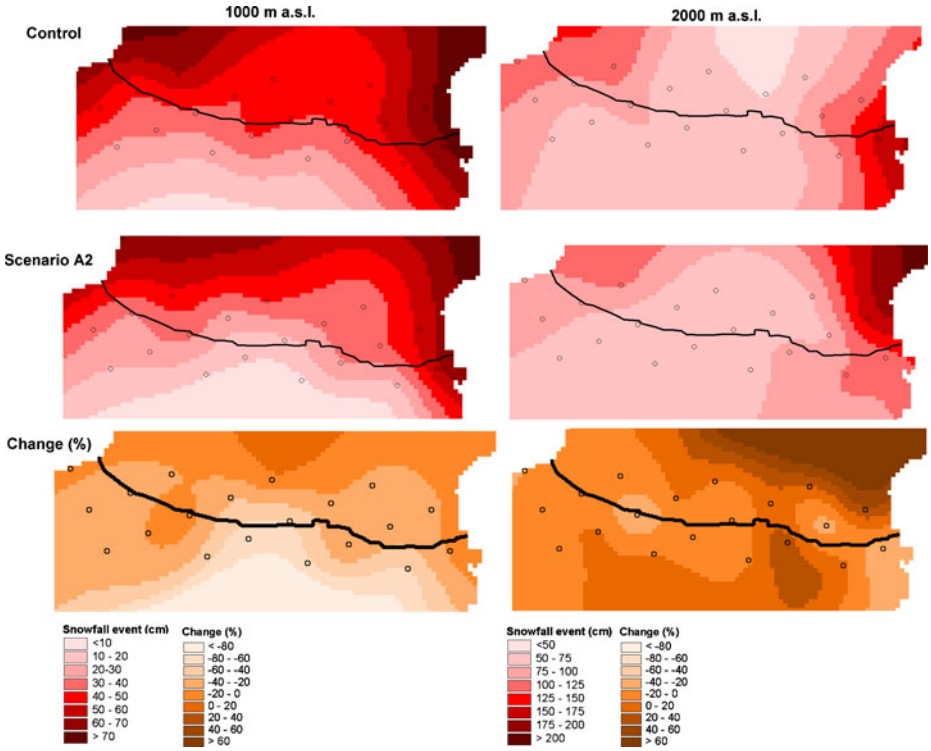

Fig. 5 Spatial distribution of 25-year quantile for the maximum intensity of snowfall for the control period and the A2 emission scenario at 1,000 and 2,000 m a.s.l. (extrapolated values may contain uncertainties beyond the 20 HIRHAM points)

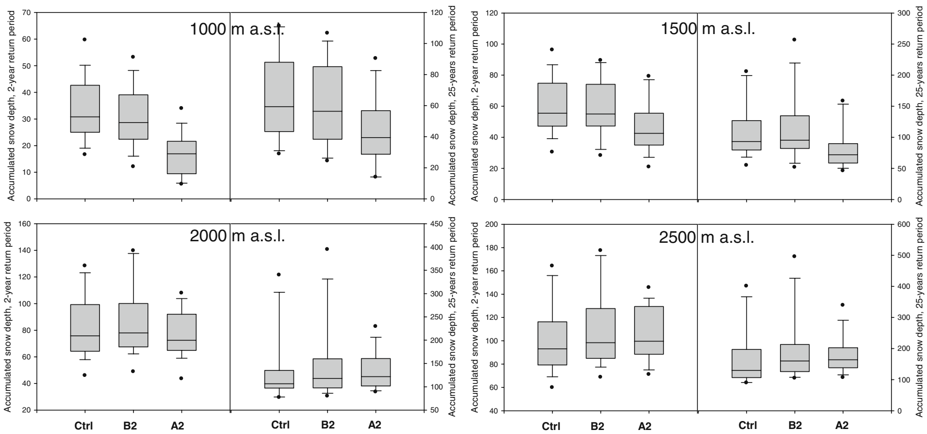

Fig. 6 Box plots for the 2-year and 25-year quantiles of the accumulated snowfall in events at various elevations for the control period and for the B2 and A2 emission scenarios. The *central line* indicates the average of the 20 analyzed grid points. *Boxes* indicate the 25 and 75 percentiles, *whiskers* indicate the 10 and 90 percentiles, and *dots* indicate the 5 and 95 percentiles

magnitude of accumulated snow in the 2-year and 25-year quantiles only occurs below 2,000 m a.s.l., and is generally more evident for the most extreme events (25-year quantile) and scenario A2. The frequency of extreme snow accumulation events is likely to remain stationary, but may increase by up to 16% at higher elevations. Figure 7 shows that the maximum accumulated snow during a multi-day snowfall event will rarely exceed 50 cm in 25 years at 1,000 m under A2 conditions, in contrast to the control period where this level of accumulation was exceeded over most of the area. The greatest changes (reductions by as much as 74%) were simulated in central and eastern areas of the Spanish Pyrenees, whereas an almost stationary evolution is expected in southwestern and northwestern areas. Under the A2 scenario, at 2,000 m a.s.l. a large area is expected to accumulate more than 150 cm in a single multi-day snowfall event in a 25-year period relative to the control period. Major increases (around 15%) are likely to occur in the central part of the French Pyrenees, whereas accumulation is expected to remain stationary or decrease in eastern areas.

Figure 8 shows that simulated changes in the frequency of HSEs will follow a similar pattern to that observed for intensity. Table 2 shows the percentage change

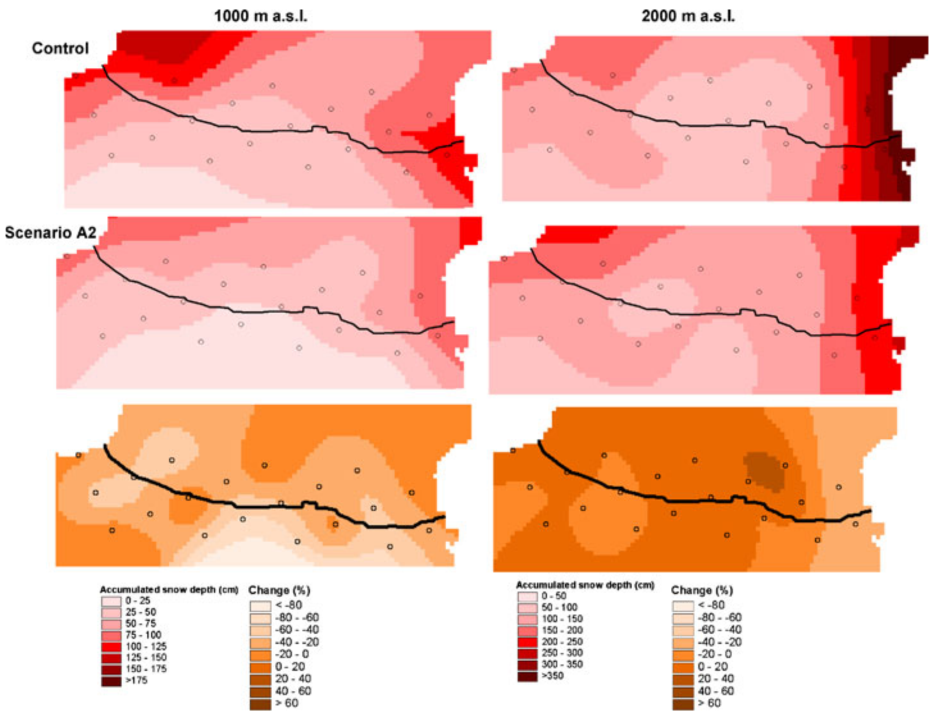

Fig. 7 Spatial distribution of the 25-year quantile for the accumulated snow during a multi-day snowfall event for the control period and the A2 emission scenario at 1,000 and 2,000 m a.s.l. (extrapolated values may contain uncertainties beyond the 20 HIRHAM points)

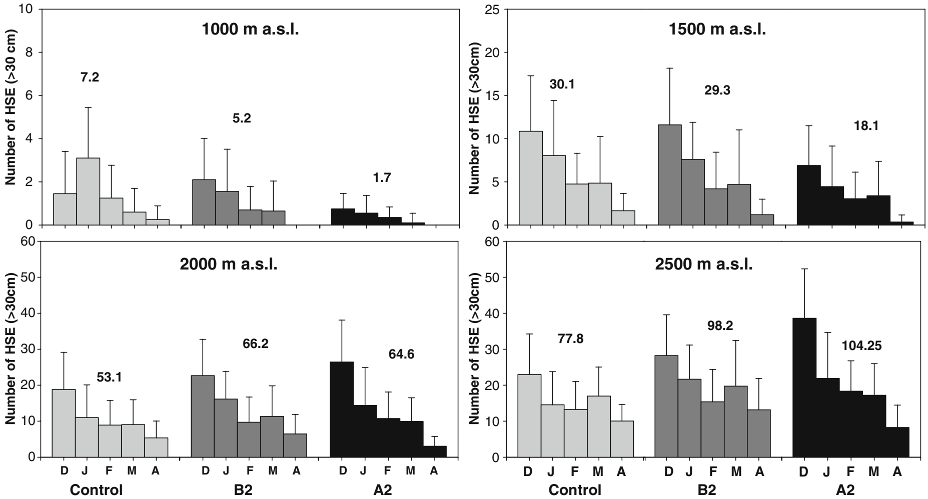

Fig. 8 Frequency of heavy snowfall events (HSE; snowfall >30 cm) in the control period and for the B2 and A2 emission scenarios. The *bars* are the average of the 20 grid points, and the *whiskers* show one standard deviation

for each month and for the period December-April. At 1,000 m a.s.l., HSEs will decline from an average of 7.2 days to 5.2 and 1.7 days for the B2 and A2 scenarios, respectively, which represents a decrease of 75% for the stronger warming scenario (A2). At this elevation the decrease may exceed 80% under A2 scenario conditions in January and March. No HSEs are expected in April under either emission scenario. For 1,500 m a.s.l., 30.1 HSEs were simulated for the control period between December and April. The number was similar for the B2 scenario (29.3) but only 18.1 (a decrease of 39.8%) for the A2 scenario; April showed the greatest decrease (27% and 78.8% for the B2 and A2 scenarios, respectively). For 2,000 m a.s.l., the expected HSEs for the B2 and A2 scenarios (66.2 and 64.6, respectively) exceeded the simulated number for the control period (53). The greatest increase is expected for December (76.9 and 47.3 for the B2 and A2 scenarios, respectively). April continues to exhibit marked decreases of −11.3% and −15% for the B2 and A2 scenarios, respectively. For 2,500 m a.s.l., an average of 77.8, 98.2 and 104.2 HSEs were simulated for the control period, and the B2 and A2 scenarios, respectively, translating to an increase of 17.6% and 22.2%, respectively. As for 2,000 m a.s.l., December showed the greatest increase (55.4% and 87.3% for the B2 and A2 scenarios, respectively), and April showed a continuing decline in HSEs under future climatic conditions.

Figure 9 shows that the results for HAEs were practically identical to those described for HSEs. Below 2,000 m a.s.l. the number of HAEs tend to decrease under both emission scenarios, with a very marked decrease (−78.4%) at 1000 a.s.l. for A2 scenario conditions. The number of simulated HAEs is expected to increase above 2,000 m a.s.l. As occurred for HSEs, the maximum increase in HAEs is expected to occur in December, whereas the greatest decrease was simulated in April.

Table 2 Percentage of change in the number of days with a snow fall accumulation of more than 30 cm (HSE) and number of events accumulating more than 60 cm (HAE) at different elevation under B2 and A2 scenarios

	Altitude (m a.s.l.)	B2 D	J	F	M	A	Tot.	A2 D	J	F	M	A	Tot.
HSE	1,000	7.6	−48.3	−45.5	−9	−100	−30	−61.5	−81.6	−72.7	−86.2	−100	−75
	1,500	6.9	−5.6	−11.6	−3.1	−27	−2.81	−36.4	−44.7	−35.8	−29.9	−78.8	−39.8
	2,000	20.5	46.8	8.9	24.9	20.6	24.7	40.7	30.1	20.8	9.9	−42	21.6
	2,500	22.8	48.8	16.2	16.2	30.8	26.1	67.8	50.2	38.5	1.2	−17.9	33.9
HAE	1,000	150	−6.2	−76.4	−25	−100	−11	−87.5	−62.5	−88.2	−75	−100	−78.4
	1,500	68	−25.6	−50	−29	−80	−11.9	−42.6	−69.2	−62.1	−38.7	−75	−55.1
	2,000	76.9	26.7	−17.2	37.6	−11.3	30.2	47.3	5.3	−13.9	2.9	−15	11
	2,500	55.4	30.6	−16.7	6.6	−9	17.6	87.3	17.9	−0.9	−15.2	−7.6	22.2

Results appear at monthly basis and the total of the period December–April. The results correspond to an average of the 20 points analyzed

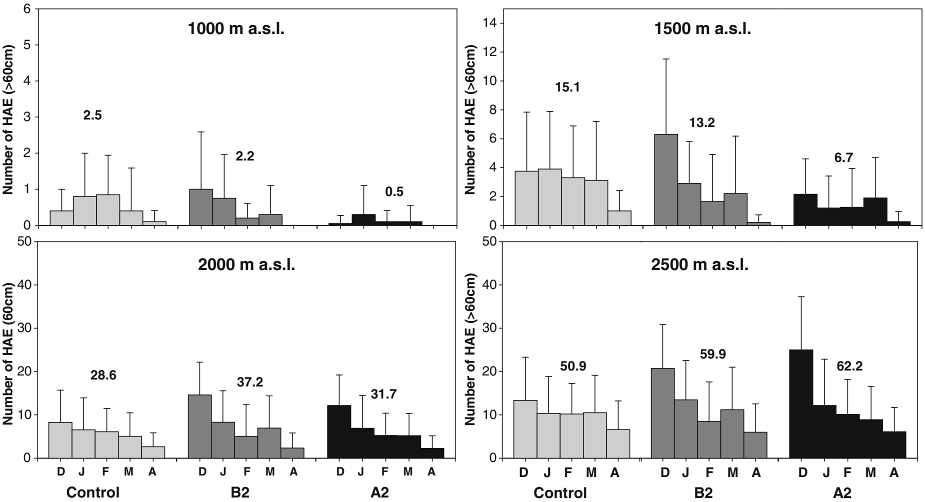

Fig. 9 Frequency of heavy accumulation events (HAE; accumulation >60 cm) in the control period and for the B2 and A2 emission scenarios. The *bars* are the average of the 20 grid points, and the *whiskers* show one standard deviation

5 Discussion

In this study we analyzed the frequency and intensity of projected HSEs by the end of the twenty-first century in comparison with those projected by simulations available for the control period (1960–1990) using the GRENBLS snow model driven by HIRHAM model outputs. Despite the marked decrease in snow accumulation and snow cover duration projected by different regional climate models for the Pyrenees (López-Moreno et al. 2009), HSEs will constitute an ongoing risk in many areas. This finding is consistent with observed climate and snow process evolution in the Alps and USA, where warming temperatures have generally reduced the amount of accumulated snow on the ground, but damaging snowstorms have increased in size and intensity (Laternser and Scheebeli 2003; Changnon 2007). Previous studies of the impacts of climate change in the Pyrenees project a mean increase in winter temperature of 1.7–2.6°C for the region (López-Moreno et al. 2008a), which may lead to an increase in liquid precipitation rather than snowfall (Kim 2005). However, RCM simulations suggest that precipitation in the Pyrenees will be concentrated in fewer days but at greater intensity (López-Moreno and Beniston 2009), which may explain a higher incidence of HSEs. Consequently, Strasser (2008) has suggested that the predicted variability in climatic extremes may lead to more frequent heavy snowfall in the Bavarian region.

Assessment of projected changes at different elevations indicated marked altitudinal gradients in the expected intensity and magnitude of future snowfall events. Thus, the simulation for 1,000 m a.s.l. suggests a marked decrease in the frequency and intensity of HSEs for both the B2 and A2 scenarios. For 1,500 m a.s.l., a decline is only expected under the scenario for the greatest greenhouse gas emissions (A2). At 2,000 m a.s.l. and higher elevations, no change or heavier snowfalls are expected under the B2 and A2 scenarios. A robust relationship between elevation and the sign of change in heavy snowfall has also been observed in the Swiss Alps, where a marked decrease in heavy snowfall below 650 m a.s.l. has been observed since 1960, and stationary or increasing trends have been detected at higher elevations (Laternser and Scheebeli 2003; Beniston 2003). The increase in heavy snowfall in areas of the Pyrenees, accompanied by increasing temperatures, may exacerbate the risk associated with large accumulations of snow. Thus, warmer temperatures may increase the humidity of the snowpack, resulting in an increase in total load (Strasser 2008). Moreover, warm winter periods and rainfall onto snow are expected to increase in frequency in coming decades (Beniston 2005; Ye et al. 2008); this may lead to rapid melting of new snow, triggering increased snow avalanches and floods in mountain rivers (Kim 2005; Germain et al. 2009).

The snowpack model produced indicators of HSEs that were largely consistent with those for the control period. However, a number of important uncertainties are associated with climate models, particularly related to precipitation extremes, posing difficulties for simulation (Frei et al. 2003; Giorgi 2005), and a robust validation cannot be easily achieved. Probably, a replication of the analysis with others RCMs dataset will lead to similar results in sign (López-Moreno et al. 2008b), but different numbers in terms of magnitude of the change. As the main objective of the paper is not to provide a precise forecast of snow events in the future (an impossible task with the current uncertainties in climatic simulations), the paper aims to broadly demonstrate how heavy snow events may change in a “greenhouse climate”. Thus, the results should be interpreted with caution and revised in the light of further progress in the understanding of the relationships between climatic variables and their feedbacks, and with the introduction of new fine-scale parameters in future climate simulations.

6 Conclusions

In this study, indicators related to HSEs for the end of the twenty-first century have been computed using an Energy Balance Model (GRENBLS) driven by atmospheric outputs from a Regional Climate model (HIRHAM). Indicators related to HSEs from RCM outputs are effective in simulating intense snowfall events when compared with observed snowpack evolution in the study area. However, caution in interpretation is required as a consequence of several sources of uncertainty. The observed changes in several variables (intensity of maximum snowfall in a single day, the accumulation of snow in multi-day snowfall events, and the number of days and periods of heavy snowfall) were very similar, enabling common conclusions to be derived. Elevation and the greenhouse gas emission scenario largely determined the expected changes in heavy snowfall by the end of the twenty-first century. Thus, for the highest emission scenario (A2), heavy snowfall intensity and frequency is expected to decrease at 1,000 and 1,500 m a.s.l. The maximum intensity of single and multi-day events is expected to decline by approximately 60% at the lower elevation, and the frequency may decline more than 80%. At 2,000 and 2,500 m a.s.l., the maximum intensity of single and multi-day events is expected to remain stationary, but may increase up to 30% at the higher elevation. The frequency is also expected to increase 11% and 22%, respectively. For a more moderate emission scenario (B2), the expected decrease in the maximum intensity at 1,000 m a.s.l. is much more moderate than under A2 conditions, and never exceeds 10%. The frequency is expected to decline by 30% for single day events, and 11% for multi-day events. At 1500 m and above an upward trend in the maximum intensity and frequency of snowpack is expected, and the frequency of HSEs may increase 20–30% above 2,000 m.

Despite the relatively small spatial scale of this study, the results indicate substantial spatial variability in the impacts of climatic change on heavy snowfall. At the lowest elevation considered (1,000 m a.s.l.), a major decrease in snowfall intensity is expected in central and eastern areas of the Spanish Pyrenees. At 2,000 m a.s.l., the major increases in intensity are expected in the central Pyrenees, especially in some areas on the French side of the range.

Acknowledgements This study was supported by the PROBASE projects CGL2006–11619 and CGL2008–01189/BTE, both financed by the Spanish Commission of Science and Technology (Ministry of Education and Science), "La nieve en el Pirineo Aragonés y su respuesta a la variabilidad climática" financed by "Obra Social La Caixa" and the Aragón Government, and the EU FP7 project ACQWA (Assessing Climatic Change and Impact on the Quantity and Quality of Water). Authors thank to PRUDENCE project for the free access to the collection of climate model outputs.

References

Barnett TP, Adam JC, Lettenmaier DP (2005) Potential impacts of a warming climate on water availability in snow-dominated regions. Nature 438:303–309

Beguería S (2005) Uncertainties in partial duration series modelling of extremes related to the choice of the threshold value. J Hydrol 303:215–230

Beguería S, Vicente-Serrano SM, López-Moreno JI, García-Ruiz JM (2009) Annual and seasonal mapping of peak intensity, magnitude and duration of extreme precipitation events across a climatic gradient, North-east Iberian Peninsula. Int J Climatol 29:1759–1779

Beniston M (2003) Climatic Change in mountain regions: a review of possible impacts. Clim Change 59:5–31

Beniston M (2005) Warm winter spells in the Swiss Alps: strong heat waves in a cold season? A study focusing on climate obsrvations at the Saentis high mountain site. Geophys Res Lett 32:L01812

Beniston M (2006) The August 2005 intense rainfall event in Switzerland: not necessarily an analog for strong convective events in a greenhouse climate. Geophys Res Lett 33:L5701

Beniston M, Keller F, Goyette S (2003) Snow pack in the Swiss Alps under changing climatic conditions: an empirical approach for climate impacts studies. Theor Appl Climatol 74:19–31

Berberan-Santos MN, Bodrenov EN, Pogliani L (1997) On the barometric formula. Am J Phys 65:404–412

Boone M, Etchevers P (2001) An inter-comparison of three snow schemes of varying complexity coupled to the same land-surface and macroscale hydrologic models. Part I: local scale evaluation at an alpine site. J Hydrometeorol 2:374–394

Brun E, David P, Sudul M, Brunot G (1992) A numerical model to simulate snow-cover stratigraphy for operational avalanche forecasting. J Glaciol 38:13–22

Brun E, Martin E, Spiridonov V (1997) The coupling of a multilayered snow model with a GCM. Ann Glaciol 25:66–72

Carrivick JL, Brewer TR (2004) Improving local estimations and regional trends of glacier equilibrium line altitudes. Geogr Ann 86a:67–79

Changnon SA (2007) Catastrophic winter storms: An scalating problem. Clim Change 84:131–139

Changnon SA, Changnon D (2006) A spatial analysis of damaging snowstorms in the United States. Nat Hazards 37:373–389

Christensen OB, Christensen JH, Machenhauer B, Botzet M (1998) Very high-resolution regional climate simulations over Scandinavia-present climate. J Climate 11:3204–3229

Cuadrat JM, Saz MA, Vicente-Serrano SM (2007) Atlas Climático de Aragón. Gobierno de Aragón, p229

Dankers R, Christensen OB (2005) Climate change impact on snow coverage, evapotranspiration and river discharge in the subartic tana basin, northern fennoscandinavia. Clim Change 69: 367–392
Datla S, Sharma S (2008) Impact of cold and snow on temporal and spatial variations of highway traffic volumes. J Transp Geogr 16:358–372
Esteban P, Jones PD, Martin-Vide J, Mases M (2005) Atmospheric circulation patterns related to heavy snowfall days in andorra, Pyrenees. Int J Climatol 25:319–329
Etchevers P, Martin E, Brown R, Fierz C, Lejeune Y, Bazile E, Boone A, Dai YJ, Essery R, Fernandez A, Gusev Y, Jordan R, Koren V, Kowalczyk E, Nasonova NO, Olga N, Pyles RD, Schlosser A, Shmakin AB, Smirnova TG, Strasser U, Verseghy D, Yamazaki T, Yang ZL (2003) Validation of the energy budget of an alpine snowpack simulated by several snow models (SnowMIP project). Ann Glaciol 38:150–158
Frei C, Christensen JH, Dequé M, Jacob D, Jones RG, Vidale PL (2003) Daily precipitation statistics in regional climate models: evaluation and intercomparison for the European Alps. J Geophys Res 108(D3):4124
Frei C, Schöll R, Fukutome S, Schimidili J, Vidale PL (2006) Future change of precipitation extremes in Europe: intercomparison scenarios from regional climate models. J Geophys Res 111:D06105
Gao X, Pal JS, Giorgi F (2006) Projected changes in mean and extreme precipitation over the Mediterranean region from a high resolution doubled nested RCM simulation. Geoph Res Lett 33:L03706
García-Ruiz JM, Puigdefabregas J, Creus J (1986) La acumulación de la nieve en el Pirineo Central y su influencia hidrológica. Pirineos 127:27–72
Germain D, Filion L, Hétu B (2009) Snow avalanche regime and climatic conditions in the Chic-Choc Range, eastern Canada. Clim Change 92:141–167
Giorgi F (2005) Climatic change prediction. Clim Change 73:239–265
Hallcross D (1997) Handbook of psychometric charts-humidity diagrams for engineers. Blackie Academic & Professional, London, p316
Hantel M, Hirtl-Wielke LM (2007) Sensitivity of Alpine snow cover to European temperature. Int J Climatol 27(10):1265–1275
Hershfield DM (1973) On the probability of extreme rainfall events. Bull Am Meteorol Soc 54:1013–1018
Höller P (2009) Avalanche cycles in Austria: an analysis of the major events in the last 50 years. Nat Hazards 48(3):399–424
Hosking JRM (1990) L-moments: analysis and estimation of distributions using linear combinations of order statistics. J R Stat Soc B 52:105–124
Hosking JRM, Wallis JR (1987) Parameter and quantile estimation for the Generalized Pareto distribution. Technometrics 29:339–349
IPCC (2007) IPCC Fourth assessment report: the physical science basis. Cambridge University Press, Cambridge, p996
Jansson P-E, Karlberg L (2001) Coupled Heat and Mass Transfer Model for Soil–Plant–Atmosphere Systems, Royal Institute of Technology, Department of Civil and Environmental Engineering, Stockholm, p321
Jonas T, Geiger F, Jenny H (2008a) Mortality pattern of the Alpine Chamois: the influence of snow-meteorological factors. Ann Glaciol 49:56–62
Jonas T, Rixen C, Sturm M, Stöckli V (2008b) How alpine plant growth is linked to snow cover and climate variability. J Geophys Res 113:G03013. doi:10.1029/2007JG000680
Julian-Andrés A, Peña-Monné JL, Chueca-Cía J, Lapeña-Laiglesia A, López-Moreno JI, Zabalza J (2000) Cartografía de zonas probables de aludes en el pirineo aragonés: metodología y resultados. Boletín de la A.G.E (Bulletin of Spanish Geographical Society) 30:119–134
Keller F, Goyette S (2005) Snowmelt under different temperature increase scenarios in the Swiss Alps. In: Dejong C, Collins DN, Ranzi R (eds) Climate and hydrology of mountain areas. Hoboken, Wiley, p315
Keller F, Goyette S, Beniston M (2005) Sensitivity analysis of snow cover to climate change scenarios and their impact on plant habitats in alpine terrain. Clim Change 72:299–319
Kim J (2005) A projection of the effects of the climate change induced by increased CO2 on extreme hydrologic events in the western U.S. Clim Change 68:153–168
Lasanta T, Laguna Marín-Yaseli M, Vicente-Serrano SM (2007) Do tourism-based ski resorts contribute to the homogeneous development of the Mediterranean mountains? A case study in the Central Spanish Pyrenees? Tour Manage 28(5):1326–1339

Laternser M, Scheebeli M (2003) Long-term snow climate trends of the Swiss Alps. Int J Climatol 23:733–750
López-Moreno JI (2005) Recent variations of snowpack depth in the Central Spanish Pyrenees. Artic, Antartic, and Alpine Research 37(2):253–260
López-Moreno JI (2006) Cambio ambiental y gestión de embalses en el Pirineo Central Español. Consejo de Protección de la Naturaleza de Aragón. Zaragoza, p260
López-Moreno JI, Beniston M (2009) Daily intensity precipitation for the 21st century: seasonal changes over an Atlantic-Mediterranean gradient in the Pyrenean mountains. Theor Appl Climatol 95:375–384
López-Moreno JI, Vicente-Serrano SM, Lanjeri S (2007) Mapping the snowpack distribution over large areas using GIS and interpolation techniques. Clim Res 33:257–270
López-Moreno JI, Goyette S, Beniston M (2008a) Climate change prediction over complex areas: spatial variability of uncertainties and expected changes over the Pyrenees from a set of regional climate models. Int J Climatol 28(11):1535–1550
López-Moreno JI, Goyette S, Beniston M, Alvera B (2008b) Sensitivity of the snow energy balance to climatic changes: implications for the evolution of snowpack in the Pyrenees in the 21st century. Clim Res 36:206–217
López-Moreno JI, Goyette S, Beniston M (2009) Impact of climate change on snowpack in the Pyrenees: horizontal spatial variability and vertical gradients. J Hydrol 347:284–396
Madsen H, Rosbjerg D (1997) The partial duration series method in regional index-flood modeling. Water Resour Res 33:737–746
McClung D, Schaerer P (eds) (1993) The mountaineers. Seattle, p276
Mellander PE, Löfvenius MO, Laudon H (2007) Climate change impact on snow and soil temperature in boreal Scot pine stands. Clim Change 85:179–193
Merritt W, Alila Y, Barton M, Taylor B, Cohen S, Neilsen D (2006) Hydrologic response to scenarios of climate change in sub watersheds of the Okanagan basin, British Columbia. J Hydrol 326: 79–108
Nakicenovic N, Grübler A, McDonalds A (1998) Global energy perspectives. Cambridge University Press, Cambridge, p299
Nesje A, Dahl SO (2000) Glaciers and environmental change. Arnold, London
Perry RH, Green DW (1997) Perry's Chemical Engineers' Handbook, 7th edn. McGraw-Hill, New York, p2400
Rao AR, Hamed KH (2000) Flood frequency analysis. CRC, New York
Rasmus S, Räisänen J, Lehning M (2004) Estimating snow conditions in Finland in the late 21st century using the SNOWPACK model with regional climate scenario data as input. Ann Glaciol 38:238–244
Spreitzhofer G (2000) On the characteristics of heavy multiple-day snowfalls in the Eastern Alps. Nat Hazards 21:35–53
Strasser U (2008) Snow loads in a changing climate: new risks? Nat Hazards Earth Syst Sci 8:1–8
Uhlmann B, Goyette S Beniston M (2009) Sensitivity analysis of snow patterns in Swiss ski resorts to shifts in temperature precipitation and humidity under condition of climate change. Int J Climatol 29:1048–1055
Wash JE (1995) Long-term observations and monitoring of the cryosphere. Clim Change 31:369–394
Ye H, yang D, Robinson D (2008) Winter rain on snow and its association with air temperature in Eurasia. Hydrol Process 22:2728–2736